PORE WATER PRESSURE CHANGES IN SANDS UNDER EARTHQUAKE LOADING

T S UENG[1], M C WU[2], C Y LIN[3] And R Y YU[4]

SUMMARY

During an earthquake the pore water pressure generation in a saturated sand layer leads to the reduction of strength and even liquefaction of the soil. In this study, a model of pore water pressure generation of sand under undrained condition was developed by adapting the previously developed drained stress-dilatancy relation based on the particulate approach. The effects of water modulus, system compliance, and rebound modulus on the pore water pressure changes were discussed. This model can be used to compute the pore water pressure change in every time step under earthquake loading. Laboratory cyclic triaxial tests, and simple shear tests were performed for Ottawa sand, Taipei silty sand, and Mailiao sand to verify this model. It was found that the overall trend of pore water pressure changes predicted by the model agreed very well with the test results. According to the model the pore water pressure buildup is related to the difference between the frictional energy and the dissipated energy for the area inside the hysteresis loop of the shear stress-strain relation.

INTRODUCTION

Under an earthquake shaking, the pore water pressure in a saturated sandy soil will increase due to the tendency of the volume contraction if the drainage of the water is impeded. This results in a lower effective stress and the reduction of strength, and even the liquefaction of the sand. The phenomenon of soil liquefaction occurred during many earthquakes in the recent years (e.g., Northridge and Kobe earthquakes) and caused severe damages.

The liquefaction or the pore water pressure buildup induced by seismic shaking is closely related to the volume change of the sand in drained condition. When a sand undergoes a drained cyclic shear stress action, the sand contracts at the beginning of shearing, and as the shear strain increases, the tendency of volume reduction reduces, eventually the volume change can become dilation. The contraction or dilation tendency depends on the density and confining pressure of the sand. A large amount of volume reduction generally occurs at the reversal of shear stress. When the shear strain increases, there is again volume dilation. The sand becomes denser after every cycle of shear stress.

For a saturated sand under undrained cyclic shear stresses, the pore pressure increases at the beginning of the shearing, whereas the increase of pore pressure gets lesser as the shear strain increases, and the pore water pressure can even become reduced depending on the density of sand. At the reversal of the shear stress, the pore pressure generally increases drastically. Under cyclic shear stresses, the pore pressure increases after each cycle and the sand can reach the state of liquefaction or cyclic mobility.

[1] *Department of Civil Engineering, National Taiwan University, Taipei, Taiwan, ROC Email: ueng@ce.ntu.edu.tw*
[2] *Department of Civil Engineering, National Taiwan University, Taipei, Taiwan, ROC*
[3] *Department of Civil Engineering, National Taiwan University, Taipei, Taiwan, ROC*
[4] *Department of Civil Engineering, National Taiwan University, Taipei, Taiwan, ROC*

[Martin, Finn and Seed, 1975] based on the compatibility of volume change of soil skeleton and the pore water, developed a relation for the pore water pressure increment for each cycle of shear stress. Other researchers, e.g., [Nemat-Nasser and Shokooh, 1979], [Simcock, et al., 1983], [Davis and Berrill, 1985], [Ishihara and Towhata,

1985], and [Figueroa, et al., 1994] had also established relations between the pore water pressure generation and the dissipated energy during each cycle of shear loading based on the observations of experiment results. However, all these relations generally consider only the pore water pressure buildup after every cycle of loading but not the change of pore pressure during every time step within a stress cycle. The later is needed for the study of the liquefaction problem during earthquakes, which induce irregular shear stress cycles. It was also found that the pore pressure change at every moment could affect the behavior of sand undergoing the consecutive loading, which in turn influences the overall pore water pressure buildup, deformation, and liquefaction of the soil during an earthquake.

This study adopts the drained stress-dilatancy relationship proposed by [Ueng and Lee,1990] to develop a model for the pore water pressure generation during the undrained cyclic loading process.

PORE WATER PRESSURE GENERATION UNDER UNDRAINED CONDITION

For a saturated sand under an undrained cyclic shear loading, the total volumetric strain is the sum of the volumetric strains of solid particles and pore water. If we assume that the solid particles are incompressible, then volumetric strain of the sand

$$d\varepsilon_v = -n \cdot \frac{du}{k_w} = n \cdot \frac{d\sigma'_n}{k_w} \tag{1}$$

where n = porosity of the sand,

du = pore water pressure change,

$d\sigma'_n$ = change of effective normal stress, and

k_w = bulk modulus of pore water.

The volume change of a saturated sand under the undrained condition can be considered to include two parts:

(1) Volume change caused by the change of effective normal stress, $d\varepsilon_{vn}$,

$$d\varepsilon_{vn} = \frac{du}{k_r} = -\frac{d\sigma'_n}{k_r} \tag{2}$$

where k_r = rebound modulus of volume change of the sand structure.

(2) Volume change caused by shearing, $d\varepsilon_{vs}$, which can be considered by adopting the stress-dilatancy relation developed by [Ueng and Lee, 1990], that is,

$$\frac{\tau}{\sigma'_n} = \pm \tan\phi_\mu \pm b\left(\frac{d\varepsilon_{vs}}{d\gamma}\right) \tag{3}$$

or

$$d\varepsilon_{vs} = \frac{1}{b} \cdot \left[\frac{\tau}{\sigma'_n} - \left(\pm \tan\phi_\mu\right)\right] \cdot d\gamma \tag{4}$$

where τ = shear stress on the shearing plan,

1) σ'_n = effective normal stress on the shearing plane,
2) ϕ_μ = basic friction angle between sand grains,
3) b = a positive value related to shearing plan orientation, friction angle, and sand fabric,
4) $d\varepsilon_v$ = volumetric strain increment, and
5) $d\gamma$ = shear strain increment.

The values of $\tan\phi_\mu$ and b were found constants for every sand independent of density, method of specimen preparation, stress path, or number of stress cycles. The ± sign in equations 3 and 4 is to indicate whether the shear stress is in the positive or negative direction. Hence, the change of total volumetric strain is

$$d\varepsilon_v = d\varepsilon_{vn} + d\varepsilon_{vs} = -\frac{d\sigma'_n}{k_r} + \frac{1}{b}\cdot\left[\frac{\tau}{\sigma'_n} - \left(\pm\tan\phi_\mu\right)\right]\cdot d\gamma \tag{5}$$

Combining equations 1 and 5, we obtain

$$d\sigma'_n = \frac{1}{\left(\frac{n}{k_w}+\frac{1}{k_r}\right)}\cdot\frac{1}{b}\cdot\left[\frac{\tau}{\sigma'_n} - \left(\pm\tan\phi_\mu\right)\right]\cdot d\gamma \tag{6}$$

The change of effective stress, or pore water pressure, for a given shear strain increment becomes,

$$\Delta\sigma'_n = \int d\sigma'_n = -\Delta u = \frac{1}{\left(\frac{n}{k_w}+\frac{1}{k_r}\right)}\cdot\frac{1}{b}\cdot\int\left[\frac{\tau}{\sigma'_n} - \left(\pm\tan\phi_\mu\right)\right]\cdot d\gamma \tag{7}$$

This relationship indicates that the pore water pressure can be computed by integrating the difference between the shear stress ratio, τ/σ'_n, and $\tan\phi_\mu$ against the shear strain and multiplying the result by the coefficient composed of the soil porosity, bulk modulus of water, rebound volumetric modulus of sand structure, and the coefficient b in the stress-dilatancy relation of the sand. Figure 1 depicts the change of effective stress during a cycle of shear stress described by equation 7. It can be seen that when the value of $\tan\phi_\mu$ is larger than that of τ/σ'_n, the effective stress decreases. In other words, the pore water pressure increases. On the contrary, when $\tan\phi_\mu$ is less than τ/σ'_n, the effective stress increases, or the pore water pressure decreases. Equation 7 can be rewritten in the form of energy relation:

$$\left(\frac{n}{k_w}+\frac{1}{k_r}\right)\int\sigma'_n\cdot d\sigma'_n = \frac{1}{b}\cdot\left[\int\tau\cdot d\gamma - \int\pm\left(\sigma'_n\cdot\tan\phi_\mu\right)\cdot d\gamma\right] \tag{8}$$

Figure 1 also shows that the pore water pressure buildup is not directly related to the dissipated energy computed according to the area enclosed inside the hysteresis loop of the shear stress-strain relation but the energy pertaining to the area outside the loop between the $\tan\phi_\mu$ and the stress-strain relation. This deviates from the concept proposed previously by others, for example, [Ishihara and Towhata, 1985] and [Figueroa, et al., 1994].

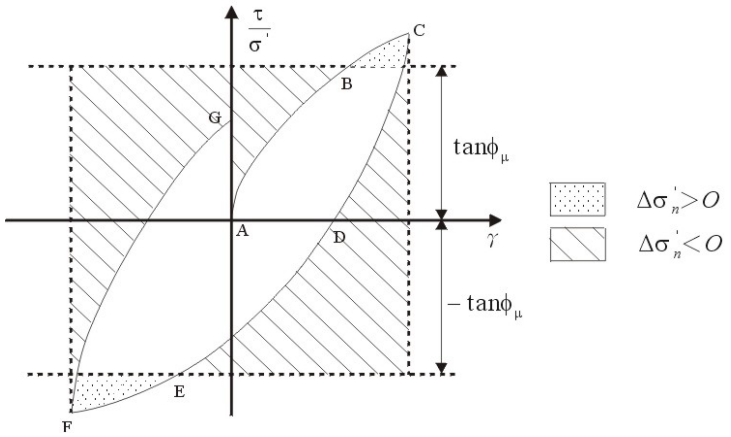

Figure 1: Shear stress ratio-strain **relation and changes of effective stress under undrained loading**

LABORATORY TESTS FOR MODEL VALIDATION

Undrained cyclic triaxial tests with constant confining pressure, undrained cyclic triaxial tests with constant mean stress, and undrained cyclic simple shear tests under constant normal stress were conducted to evaluate the proposed model. The changes of pore water pressures in the specimens were measured during the undrained cyclic loading. CKC dynamic triaxial test apparatus was used for the cyclic triaxial test and NGI simple shear device was used in the simple shear tests. In addition, isotropic consolidation tests, consolidated drained test,

oedometer consolidation tests, and drained cyclic triaxial and simple shear tests were performed. Ottawa sand (ASTM C-778), Taipei silty sand, and Mailiao sand were used in this study. The properties of these sands are shown in Table 1. Details of these tests are given in [Wu, 1997], [Lin, 1998], and [Yu, 1999].

Table 1: **Properties** of the test sands

	Ottawa sand	Taipei silty sand	Mailiao sand
G_s	2.64	2.71	2.66
D_{10}	0.2 mm	0.075 mm	0.075 mm
D_{50}	0.34 mm	0.160 mm	0.118 mm
Fines content	0	10%	10%
C_u	1.9	2.5	1.78
e_{max}	0.760	1.076	1.262
e_{min}	0.476	0.581	0.762

In the drained triaxial and simple shear tests, values of the parameters in equation 1 were determined according to the relation between the stress ratio and the dilatancy rate on the octahedral or horizontal planes, respectively (e.g., Fig. 2). The drained test results verify the stress-dilatancy relationship (equation 3) proposed by [Ueng and Lee, 1990]. It was also found that there is a unique relationship between the stress ratio, τ/σ'_n, and shear strain for these test sands under different confining pressures. Figure 3 is a typical example. Therefore, the computations of the pore water pressure generation in equation 7 can be performed without considering the change of effective stress during the loading.

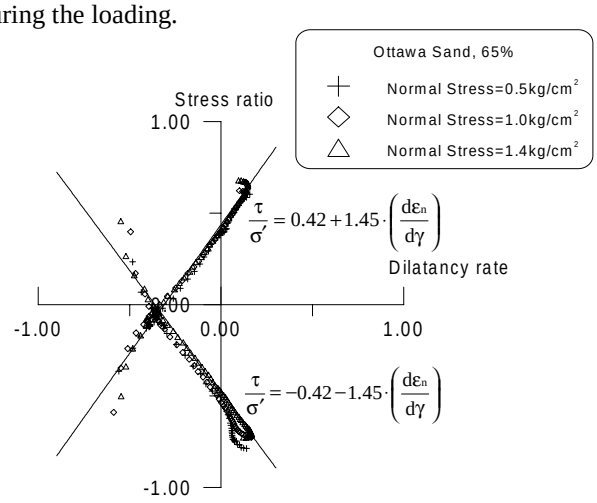

Figure: 2 Relation between shear stress ratio and dilatancy rate in simple shear test

Under undrained condition, since there is always a pore water pressure buildup, especially at the beginning of the loading, the effective stress decreases and the sand structure tends to expand. In other words, the soil is in an unloading condition. When there were pore pressure reductions during the cyclic loading, the sand should be under the stage of reloading. Therefore, the rebound/reloading moduli of volume changes, k_r, for these sands obtained in the consolidation tests (e.g., Fig. 4) were used in the computations. A constant value of kr was used in the computations, but it was found out that k_r varies with σ'_n, and the value will be quite different when the effective stress approaching zero near the stage of liquefaction. Therefore, kr was considered as a function of effective stress in the later computations.

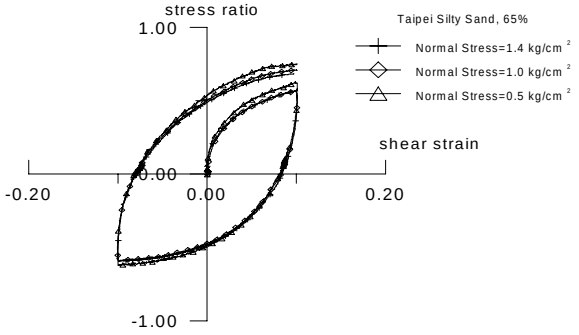

Figure 3: Stress ratio-strain relation in drained cyclic simple shear test

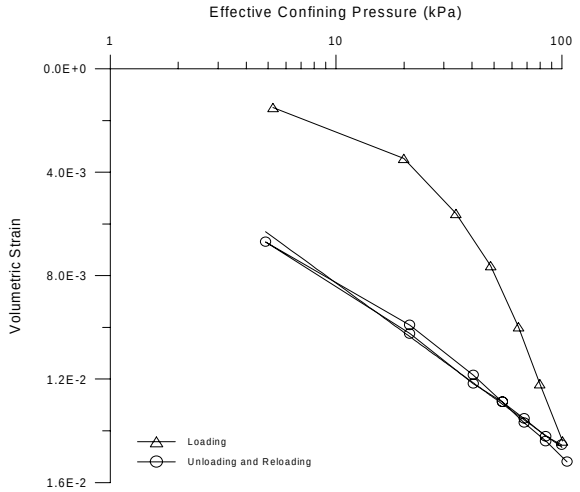

Figure 4: Relation of volumetric strain versus mean effective stress for Mailiao sand

The bulk modulus of pure water is 2.15×10^6 kPa. For the undrained tests, the bulk modulus of water, k_w, should include the effects of the degree of saturation and the compliance of the whole testing system. Therefore, k_w was computed based on the B value obtained before the cyclic tests. They are in the order of 10^5 kPa which is consistent with the values obtained by [Garga and Zhang, 1997]. The values of the parameters used in equation 7 for computations of the pore pressure changes are given in Table 2.

Table 2: Values of parameters used in model computations

	Ottawa sand				Taipei silty sand	Mailiao sand
Test	TCC	TCM	TCM	SST	SST	TCM
Dr (%)	35	50	65	65	65	40
n	0.4	0.382	0.365	0.365	0.45	0.515
b	2.09	0.91	0.91	1.45	1.61	1.39
$\tan\phi_\mu$	0.46	0.37	0.37	0.42	0.52	0.43
k_r (kPa)	65000	332 σ'	401 σ'	22900	17100	369 σ'
k_w (kPa)	3.95×10^5	2.47×10^5	2.83×10^5	4.00×10^5	3.08×10^5	0.68×10^5

Notes: TCC = triaxial test with constant confining pressure, TCM = triaxial test with constant mean stress, SST = simple shear test.

The values of k_w were computed based on the B values in the tests.

COMPARISON OF TEST RESULTS AND MODEL COMPUTATIONS

The pore water pressure changes in these sands were computed using equation 7 according to the testing conditions, and compared with the pore pressure measured in the undrained cyclic tests. In the cyclic triaxial test with constant confining pressure, the mean stress of the specimens also changed along with the application of the cyclic deviator stress. The pore pressure change due to the change of the mean stress should be deducted before the comparison was made because equation 7 does not consider the pore pressure change induced by the mean stress change.

Figure 5 is the typical results of pore water pressure change during tests and their comparisons with the results obtained according to the model. The comparison shows that the trend of pore water pressure generation agrees well between the laboratory test results and the computed results according to the model proposed in this study. The details of pore pressure changes within each load cycle are described fairly closely by the proposed model.

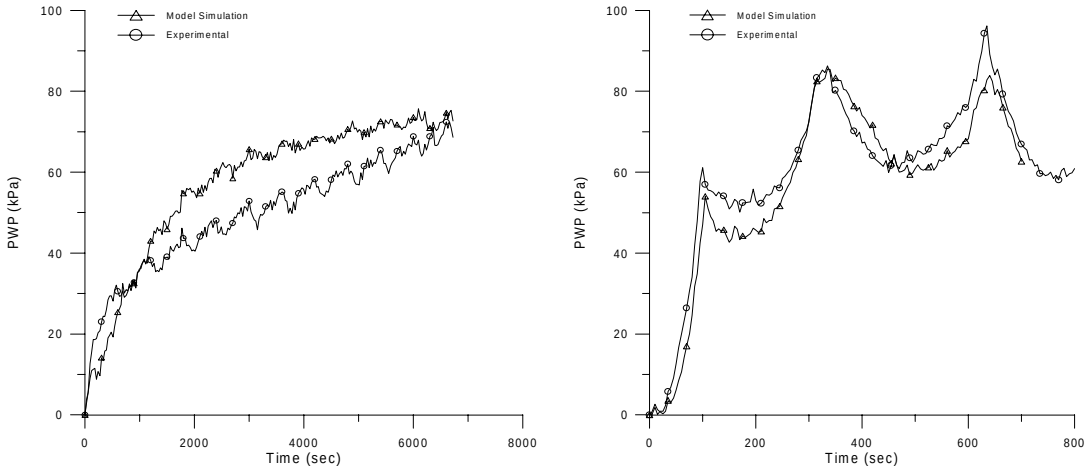

(a) Mailiao sand, Dr = 40% **(b) Ottawa sand, Dr = 65%**

Figure 5: Comparisons of pore water pressure changes between computed and measured results

It is also found that the water bulk modulus, the system compliance, and the deformability of the specimen boundaries have significant effects on the pore pressure changes in the undrained condition. The results show that when k_w is at least one order of magnitude higher than k_r, the pore water pressure generation of sands under cyclic shear loading would not significantly affected by the change of the modulus of pore water. Figure 6 shows the effect on the pore water pressure changes for various values of k_w.

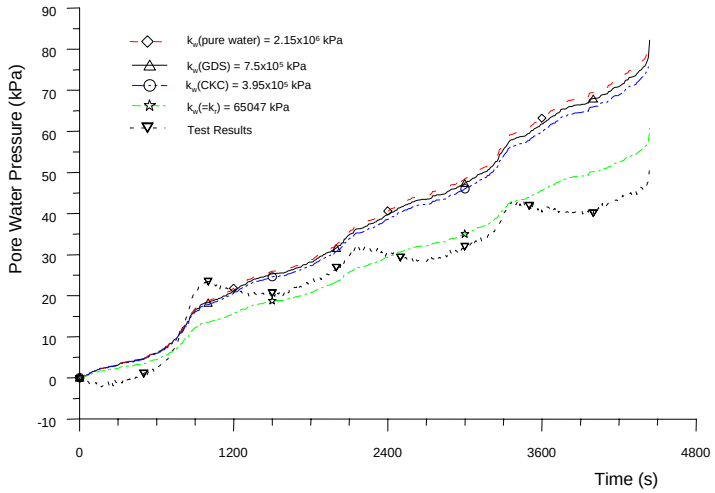

Figure 6: Effect of water bulk modulus on the pore water pressure changes

The shear stress-ratio-strain relations obtained in the undrained tests should be used in the model computations for the pore water pressure generation in sand under undrained loading. It appears that the use of the drained stress-strain relation in the model computation does not give good results for the undrained condition in which very little volume change is allowed.

CONCLUSIONS

In this study, a model of pore water pressure generation under the undrained cyclic shear loading was developed based on the stress-dilatancy relation in the drained condition. According to equation 7, the change of effective stress or the pore water pressure generation can be computed using the values of porosity, $\tan\phi_\mu$, rebound bulk modulus of volume change, coefficient b in the stress-dilatancy relation, and stress ratio-strain relation of the sand obtained in the laboratory tests. The proposed model can describe the pore water pressure change for every time step rather than that after each stress cycle during the cyclic shear loading. It is suitable for use in the consideration of the pore water pressure generation during the irregular shaking induce by an earthquake. Comparison between the computed pore pressure generation and the results of undrained cyclic tests for Ottawa

sand, Taipei silty sand, and Mailiao sand showed that this model can very well describe the process and the trend of the pore water pressure generation under cyclic loading.

ACKNOWLEDGMENT

This study is supported by the National Science Council, ROC, Grants Nos. NSC87-2621-P-002-031and NSC88-2625-Z-002-034.

REFERENCES

Davis, R.O. and Berrill, J.B. (1985), "Energy dissipation and seismic liquefaction of sands: revised model", *Soils and Foundations*, 25, 2, pp106-118.

Figueroa, J.L., Saada, A.S., Liang, L., and Dahisaria, M.N. (1994), "Evaluation of soil liquefaction by energy principles", *Journal of Geotechnical Engineering*, ASCE, 120, 9, pp1554-1569.

Garga, V.K. and Zhang, H. (1997), "Volume changes in undrained triaxial tests on sands", Canadian Geotechnical Journal, 34, pp762-772.

Ishihara, K.L. and Towhata, I. (1985), "Shear work and pore water pressure in undrained shear", *Soils and Foundations*, 25, 3, pp73-84.

Lin, C.Y. (1998), *Pore Water Generation Of Sands Under Undrained Cyclic Simple Shear Loading*, M.S. thesis, Dept. of Civil Engineering, National Taiwan University.

Martin, G.R., Liam Finn, W.D., and Seed, H.B. (1975), "Fundamentals of liquefaction under cyclic loading", *Journal of Geotechnical Engineering Div.*, ASCE, 101, GT5, pp423-437.

Nemat-Nasser, S. and Shokooh, A. (1979), "A unified approach to densification and liquefaction of cohesionless sand in cyclic shear", *Canadian Geotechnical Journal*, 16, pp659-678.

Simcock, K.J., Davis, R.O., Berrill, J.B., and Mullenger, G. (1983), "Cyclic triaxial tests with continuous measurement of dissipated energy", *Geotechnical Testing Journal*, 6, 1, pp35-39.

Ueng, T.S. and Lee, C.J. (1990), "Deformation behavior of sand under shear-particulate approach", *Journal of Geotechnical Engineering*, ASCE, 116, 11, pp1625-1640.

Wu, M.C. (1997), *Pore Water Pressure Generation of Sands Under Cyclic Loading*, M.S. thesis, Dept. of Civil Engineering, National Taiwan University.

Yu, R.Y. (1999), *Modeling of Pore Water Pressure Generation of Saturated Sands*, M.S. thesis, Dept. of Civil Engineering, National Taiwan University.